International Research Journal of Engineering and Technology (IRJET) e-ISSN: 2395-0056
Volume: 06 Issue: 05 | May 2019 www.irjet.net p-ISSN: 2395-0072

Study of Various Passive Drag Reduction Techniques on External Vehicle Aerodynamics Performance: CFD Based Approach

Basudev Datta[1,2,3,4], Vaibhav Goel[5], Shivam Garg[5] and Inderpreet Singh[5]

[1]*Plant Operation Control Intern, Maruti Suzuki India Limited-Gurgaon Plant*
[2]*MBA (Operations) Student, Symbiosis Institute of Management Studies-Pune*
[3]*Former Assistant Professor, C V Raman College of Engineering-Bhubaneswar*
[4]*Former Trainee Scientist (Scientist Gr.IV(1)), Council of Scientific and Industrial Research (Dhanbad Campus)*
[5]*B.Tech. Student, Dept. of Mechanical Engineering, Chitkara University- Rajpura*

Abstract - *Recent trend of fluctuation in fuel prices and associated concern regarding global warming due to greenhouse gas emission has attracted the engineers to think over the prevailing techniques of the improving fuel economy. Automobile engineers have already tried various techniques to improve fuel efficiency by engine and chassis weight modifications. However, the area of vehicle aerodynamics for improving fuel efficiency has caught the eyes of automobile researchers which involve reducing the magnitude of drag coefficient using various drag reduction techniques. In the present paper, an attempt has been made to improve external vehicle aerodynamics performance by exploiting various passive drag reduction techniques based on Computational Fluid Dynamics (CFD) using ANSYS Fluent v14 (Non Commercial Version) to reduce fuel consumption and in turn pollution.*

Key Words: **CFD, body of influence, realizable K-epsilon model, lift & drag coefficients**

1. INTRODUCTION

Global trend of fluctuation (most of the time increase) in fuel prices, heavy consumption of fuel by inefficient and older vehicles *(Majumder and Saha, 2014),* immense pressure of environmental regulators to control the greenhouse gases emission *(Sudin et al., 2014)* have increased the demand for design and development of fuel efficient vehicles. Fuel efficiency of vehicle can be improved by various techniques such as i) fuel efficient engine technology, ii) chassis weight reduction techniques and iii) external aerodynamic drag reduction techniques *(Rohatgi, 2012; Koike et al., 2004; Carr, 1969).* As a result, tremendous amount of research has been carried out in the field of design of efficient engines and chassis weight reduction techniques by automobile industry *(Demmler, 1998; Buchholz, 1998).* Fuel efficient engines coupled with chassis made of composite materials (e.g., carbon fibre) have improved the fuel efficiency to some extent *(Small et al., 2006)* but could not provide the satisfactory solution. It is observed that fuel consumption increases upto 50% due to aerodynamic drag *(Sudin et al., 2014).* Implementation of active and passive drag reduction techniques (*Mayer and Wickern, 2011, Hsu and Davis, 2010)* provide a cost-effective solution to improve fuel economy *(Hucho and Sovran, 1993).* In case of active drag reduction techniques, network of actuators coupled with sensor based controllers are used which make the system very complex as well as add extra weight to the vehicle effecting overall performance. However, traditional passive drag reduction techniques involve modification in external geometry of vehicles or attaching additional static devices to reduce the drag. As a result, passive drag reduction techniques are mostly preferred by automobile manufacturers due to its cost effectiveness and simplicity in design. Therefore, in the present paper, various passive drag reduction techniques have been exploited to improve external vehicle aerodynamics performance using Computational Fluid Dynamics (CFD) based approach to reduce fuel consumption and in turn pollution. Author has used noncommercial version of both ANSYS Fluent v14 & Dassualt Systeme CATIA v5r19 for simulation purpose. The second and third sections of this paper illustrate the classification of different passive drag reduction techniques and simulation set up including solver settings respectively followed by results and discussions.

2. CLASSIFICATION OF DIFFERENT PASSIVE DRAG REDUCTION TECHNIQUES

The drag can be dealt with two different perceptions in case of vehicles: i) due to vehicle and ii) due to the fluid through which vehicle travels. In accordance to Newton's Third law of motion, every action has equal and opposite reaction. Similarly, in case of fluid dynamics, due to force exerted by vehicle motion on fluid, equal and opposite resistive forces i.e. drag forces are exerted

on vehicle by fluid which tries to resist its motion. However, the drag which a vehicle exerts due to a fluid stream is the summation of pressure drag and skin friction drag *(Hucho and Sovran, 1993).* Pressure drag depends upon geometrical configuration of system due to phenomenon of boundary layer separation from the surface of rear window and formation of wake region behind the vehicle which accounts for more than 80% of the total drag (*Majumder and Saha, 2014*). In such conditions, large pressure difference is developed across front and rear section of a car. As a result, vehicle experiences a drag force in the direction of air movement. In addition to that, speed of vehicle and wake region produced due to the moving vehicle also affects the magnitude of drag *(Singh, 2004, Sudin et al., 2014).* It is general tendency that 40% of overall induced drag forces are concentrated at rear section of a car geometry *(Chainani and Perera, 2008; Sudin et al., 2014).* Though drag forces are more concerning factor, lift forces also play considerable role in improving the dynamic stability of a vehicle. Larger is the value of lift coefficient, higher is the instability of vehicle. The generation of negative lift forces is an added advantage while driving at higher speeds. For such purposes some special devices like spoilers are required to be installed. The negative lift forces increase the grip of the car tires on the road *(Ahmed and Chacko, 2012).* On the other hand, the heavy and large sized vehicles (trucks, buses etc.), design becomes aerodynamically inefficient due to large frontal area and non-streamlined body shape which consumes upto 65% additional fuel to overcome the induced drag resistance *(Altaf et al., 2014, Wahba et. al., 2012)* even if it has better tyre grip with surface. It means aerodynamic drag largely dependent on geometrical configuration of the body of a vehicle in addition to fluid flow conditions i.e., laminar or turbulent. In case of streamlined bodies (e.g. sports cars), one can reduce the drag to some extent by changing the flow conditions i.e. varying Reynolds number. But situation becomes complex in case of bluff bodies with sharp corners (buses, trucks) where Reynolds number variation has no effect on aerodynamic drag. Hence, structural modification of a vehicle is required to reduce the drag to control the flow separation *(Altaf et al., 2014).* The various structural modifications can be done by using the following techniques either individually or in combination for passive drag reduction.

2.1 Rear Tail Flaps

It is most common type of passive drag reduction techniques. Tail flaps are always installed in the rear section of the vehicle. The flaps are usually installed horizontally at the top and bottom sections of utility vehicles and vertically along sides in case of bluff body vehicles as shown in Fig. 1(a) and Fig. 1(b) respectively. Numerical investigation of vertical tail flaps on sports utility vehicles conducted by Wahba *et al.* (2012) clearly indicated that the diversion of air takes place into low pressure wake zone to reduce drag upto 18% by improving the wake pressure recovery process. Though some parameters such as crossectional area, chord length and angle of attack must be varied in such a way that vehicle aerodynamic performance is optimized (*Sudin et al., 2014).* Sudden upward deflection of air flow underneath the car causes reduction in drag coefficient by 30% due to reduced turbulent intensities in near wake zones, shortening and weakening of recirculation zones and reduction in base pressure *(Khalighi et al., 2013).* Lots of research has been carried to determine the influence of angle of attack on drag and lift coefficient to determine optimal angle of attack *(Sharma and Bansal, 2013).*Wind tunnel analysis by *Fourrié et al. (2011)* clearly shows that widening of separated zone which obstructs the process of development of counter rotating longitudinal vortices near lateral edges of rear window causing significant reduction in magnitude of drag.

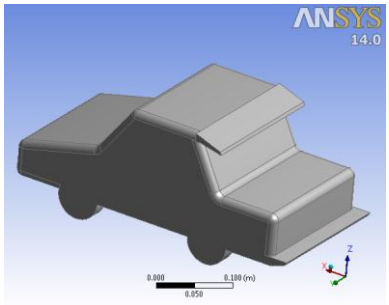

(a) Horizontal tail flaps at 20° angle of attack installed in rear section of passenger car

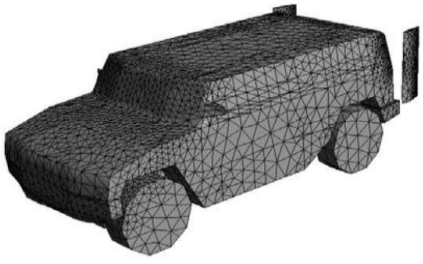

(b) Vertical tail flaps installed in rear section of SUV *(Wahba et al., 2012).*

Fig. 1: Different installation techniques of rear tail flaps for utility and bluff body vehicles

2.2 Ground Effect

Air flow across the car body with abrupt change in geometrical shape causes development of abnormal high pressure zones. Due to development of high pressure zone in the car roof, significant amount of downward force is exerted on undercarriage i.e. in low pressure zone *(Ahmed and Chacko, 2012).* Since the ground effect techniques is based on Bernoulli's principle, therefore, it is suggested to reduce frontal ground clearance area as depicted in Fig 2(b). It causes the air velocity to increase gradually producing low pressure zones underneath the car i.e. undercarriage section of a car. The entire process not only reduces the drag coefficient but also improves the vehicle dynamic stability. Dynamic stability of a car is improved due to addition of negative forces to tyre gripping force which counters the lift forces developed.

2.3 Diffuser

It is well known fact that high exit velocity of air underneath the rear section of a vehicle causes widening of flow separation. Recirculation of air due to difference in pressure across upstream and downstream at rear section of a car causes increment in induced drag. In order to avoid the same, diffuser technique is used *(Ahmed and Chacko, 2012)*. It involves certain modification of underbody/undercarriage tray of the car especially, in the rear section as illustrated in Fig 2(c) *(Katz, 2006)* so as to prevent the re-circulation of air at rear section by restoring air velocity at exit point.

Various researchers have done different modifications to utilize diffuser technique. *Mazyan (2013)* modified front head with rear wings which reduced the coefficient of drag by 21%. *Marklund et al. (2013)* studied the influence of ground proximity of underbody tray and diffuser angle on drag coefficient based on flow physics and wake analysis for Sedan passenger car with low ground clearance. They found that coefficient of drag is reduced by 2-3%. Modification of underbody tray shape was done similar to venturi nozzle without endplates to reduce drag *(Huminic et al., 2012).* CFD simulation by *Sudin et al. (2014)* indicates that drag coefficient reduces by 4% when movable arc-shaped semi-diffuser devices in underbody tray is installed in order to facilitate streamlined flow of air. Therefore, it can be concluded that the area of crossection exposed to the incoming air flow may be increased gradually at particular slant angle to minimize the recirculation.

2.4 Vortex Generator

It is a small vane shaped aerodynamic surface used in aerospace sector that produces vortices in the air flow. Such devices are mostly installed at the top end of rear section of a car just before declination of rear wind screen of the car as shown in Fig. 2(d). It is an inherent property of the vortex generator to induce drag initially. However, at the same time it reduces more drag in comparison to the initially induced drag by delaying flow separation at the downstream side *(Dubey et al., 2013)*. The purposes of vortex generator are: i) to control the boundary layer transition and ii) to delay the flow separation to generate the strong negative lift forces thereby improving dynamic stability of a car *(Ahmed and Chacko, 2012)*. It works on the principle of exchange of momentum between upstream and downstream flows. Downstream air pressure increases with respect to upstream at rear end due to tapered shape of vortex generators. As a result, a resisting force is generated in opposite direction. The phenomenon of delay in flow separation at the roof of the rear section of Sedan and Hatchback is tested using GAMBIT and FLUENT after installation of bump shaped vortex generators. CFD analysis data indicates that both lift and drag coefficient can be reduced by installing vortex generator at the rear section of the car *(Koike et al. 2004).*

2.5 Front Bonnet Duct

In order to minimize the coefficient of drag, designers need to focus how to eliminate or minimize the high pressure zones. The high pressure zones are associated with speed of a car. It is obvious that higher is the air speed, lower is the pressure. Usually, due to sudden increase in angle encountered by fluid flow with front section of a car, air speed drastically reduces resulting into generation of high pressure zones. Therefore, a front bonnet duct is generally used for this purpose as shown in Fig 2(e). The purposes are mainly: i) to reduce the high pressure zones in the front section of a car to reduce drag coefficient *(Ahmed and Chacko, 2012)* and ii) additional air cooling of engine.

2.6 Rear Spoiler

The basic design of rear spoiler is taken from the wings used in the aircrafts *(Ahmed and Chacko, 2012)*. In the aircraft industry, wings are used to generate lift forces, however, in case of automobile industry, it is used to minimize unfavorable air movement. Rear spoilers are usually inverted wings installed over the trunk lid in rear section of a car as illustrated in Fig 2(f). It has tendency to diffuse the air flowing around the vehicle, by minimizing the turbulent kinetic energy at the rear section of the car. It results into generation of large amount of negative lift forces due to development of downwards pressure *(Zakem, 2008; Daryakenari et al., 2013).* This device not only reduces the drag but also improves dynamic stability of a car. In earlier phase of development of spoilers, these were installed just for decoration purpose. But research shows that today is the need of these spoilers for reducing the drag significantly and improving the dynamic stability *(Hu et al., 2011).*

2.7 Rear Fairing

It is one of the rarely used passive drag reducing techniques. Since, it requires complete geometrical overhauling of rear section of a car influencing the aesthetics of the same. It generally involves conversion of rear section of the car into truncated cone design with rectangular or square sectional base similar to that of the tail section of an aircraft as shown in Fig. 2(g). A careful attention must be given to design the slant angle of rear fairing in order to minimize the flow separation phenomenon. Sudden change in slant angle of rear fairing must be avoided. It is reported that installation of rear fairing has reduced the drag coefficient by 26% *(Rohatgi, 2012).*

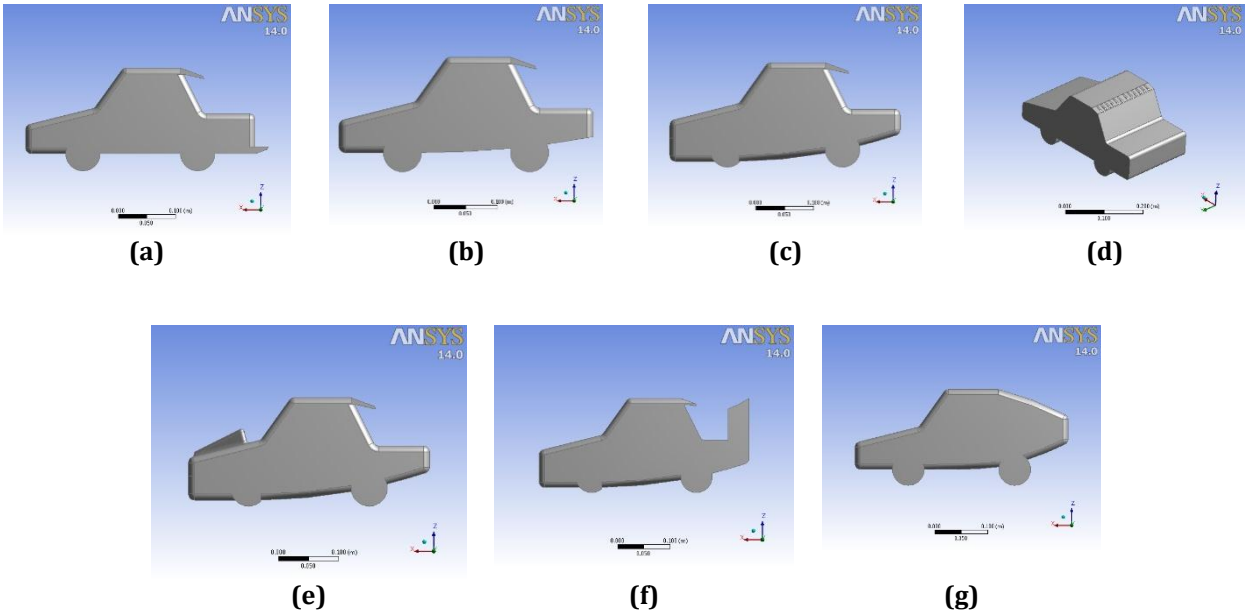

Fig 2: Various Passive drag reducing techniques installed in base model of car

(a) Rear Tail Plate, (b) Ground Effect, (c) Diffuser, (d) Vortex Generator, (e) Front Bonnet Duct, (f) Rear spoiler and (g) Rear fairing

3. MODEL DESCRIPTION

The generic model of a car was designed using Dassualt Systeme CATIA v5r19 software for the present study. It was imported to ANSYS Fluent v14 for CFD simulation purpose as shown in Fig. 3 below. Though the car was initially designed with its actual dimension as shown in Fig. 3 (base length=4m, base width=2m and height=1.8m) but the design was reduced to 1:10 scale to facilitate faster computational process.

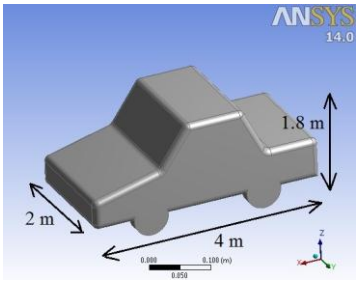

Fig 3: Dimensional specification of base model car

4. CFD SIMULATION SETUP

External Aerodynamic evaluation of air flow over a vehicle can be done using either analytical method or CFD approach. It is obvious that for solving the air flow problems, we have to compute the Navier-Stroke equation and continuity equation. Analytical methods can be used to solve air flow problems over simple geometries like laminar flow over a flat plate. However, in case of complex fluid flow i.e. turbulent flow over bluff bodies, it is almost impossible to solve analytically both Navier-Stroke equation and continuity equation even using latest version of computers due to large computational time. To reduce the same, a time averaged Navier-Stokes equation along with turbulent models is used.

In the present study, CFD simulation is carried out using Viscous realizable K-Ɛ Turbulence Model (2 equations) with Non-equilibrium wall function as near wall treatment. The model used in current study is very robust with reasonable computational time and widely used by automobile designers. Steps of CFD Analysis involves: (i) Selection of base model of the vehicle, (ii) Designing the base model of vehicle using Dassualt Systeme CATIA v5r19, (iii) Applying boundary conditions for CFD Simulation on base model of vehicle in ANSYS Fluent v14, (iv) Generation of virtual wind tunnel environment using ANSYS Fluent v14, (v) Determination of lift and drag coefficient of base model of vehicle using ANSYS Fluent v14 and (vi) Determination of lift and drag coefficient of base model of vehicle with passive drag reduction technologies installed using ANSYS Fluent v14.

The base model of the car in this paper have symmetrical geometry. Hence, symmetrical fluid flow field has been taken into consideration for numerical simulation purpose *(Xingjun et al., 2011; Xingjun et al. 2010; Majumder and Saha, 2014).* In order to further minimize the computational time and resources, more refined mesh and half of the base model car is used for CFD Simulation. Since, the computational domain is a general requirement for any external fluid flow analysis which is defined as a box/spherical/cylindrical shaped domain surrounding the structure depending upon type of structure to be evaluated. In case of cars, box shaped domain is preferred which is filled with fluid and has boundaries defining the characteristics of fluid flow as illustrated in Fig. 4.

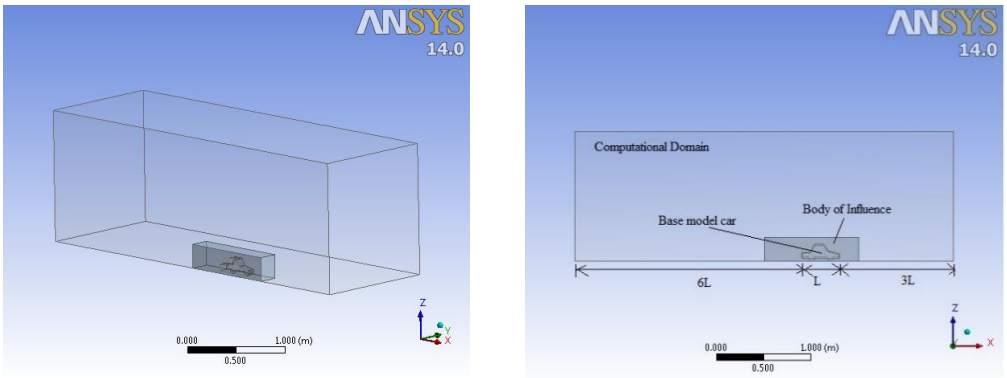

(a) **(b)**

Fig 4: Computational domain of Base model car (a) Isometric View and (b) Side View

Recent trends in CFD simulation indicates that size of computational domain is one of the important factors. It is needed to facilitate efficient computation and capture the details regarding change in fluid flow characteristics. In general, keeping in view

the Length of a car=L, 2L, 3L and 6L have been taken as size of computational domain (*Majumder and Saha, 2014)* on lateral sides, upstream and downstream sides of the car, respectively. The complete model was meshed using ANSYS Fluent v14 which is essentially composed of tetrahedral and prismatic meshes as shown in Fig. 5. Prismatic meshing was done in order to facilitate detail capturing of surface forces acting on the vehicle with accuracy. It is implemented on vehicle body, wheels and road surface. Program controlled inflation was inserted on the model to apply boundary layers. The best practices for meshing in external vehicle aerodynamics recommends that value of first aspect ratio, maximum number of layers and growth rate should be kept as 5, 5 and 1.2 respectively as shown in Fig. 5 while meshing (*Majumder and Saha, 2014)*. In order to capture the details regarding formation of vortices at rear section of the car, finer meshing is required. Hence, local mesh refinement was done wherever accuracy is required. Another computational domain was built around the vehicle body to refine the mesh closer to the car and coarsen the rest of domain space i.e. body of influence. Introduction of body of influence feature around the vehicle body reduces the computational effort and captures the detailed change in fluid flow characteristics. In general, dimension of body of influence is 0.5L in lateral sides, 0.5L and L in upstream and downstream directions respectively which extended by 0.5L above the roof *(Ahmad et al., 2010; Skaperdas and Kolovos, 2009).*

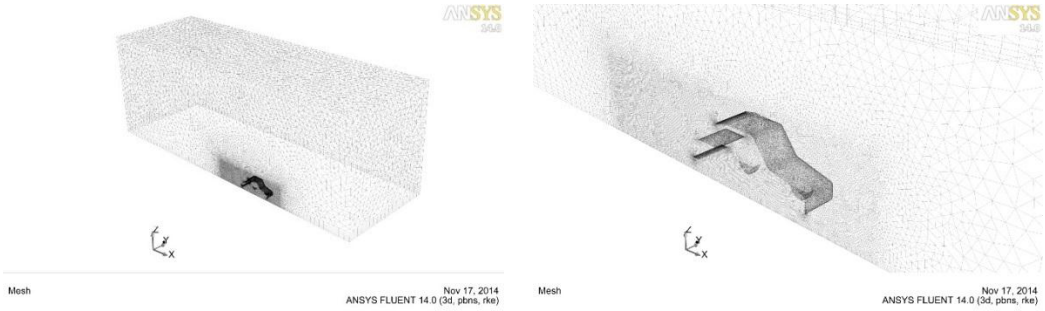

(a) **(b)**

Fig 5: Meshing in ANSYS Fluent v14
(a) Grid Topology and (b) Tetrahedral mesh and Prism Layers

4.1 Solver Setting

ANSYS Fluent v14 CFD solver is used for numerical simulation of vehicle external aerodynamics to evaluate the performance of different passive drag reduction techniques. Fluent solver uses Navier-strokes equations which are composed of continuity and momentum equations as discussed below in Eqns. (1) and (2).

Continuity Equation:

$$\frac{\partial u}{\partial x} + \frac{\partial v}{\partial y} + \frac{\partial w}{\partial z} = 0 \qquad (1)$$

Momentum equations:

$$u\frac{du}{dx} + v\frac{du}{dy} + w\frac{du}{dz} = -\frac{1}{\rho}\frac{\partial p}{\partial x} + \frac{1}{\rho}(\partial\tau_{xy}/\partial y + \partial\tau_{xz}/\partial z) + B_x \qquad (2a)$$

$$u\frac{dv}{dx} + v\frac{dv}{dy} + w\frac{dv}{dz} = -\frac{1}{\rho}\frac{\partial p}{\partial y} + \frac{1}{\rho}(\partial\tau_{xy}/\partial x + \partial\tau_{yz}/\partial z) + B_y \qquad (2b)$$

$$u\frac{dw}{dx} + v\frac{dw}{dy} + w\frac{dw}{dz} = -\frac{1}{\rho}\frac{\partial p}{\partial z} + \frac{1}{\rho}(\partial\tau_{xz}/\partial x + \partial\tau_{yz}/\partial y) + B_x \qquad (2c)$$

Some assumptions are made for simulation set up which are: i) steady state inlet air velocity, ii) zero degree yaw angle, iii) constant pressure at outlet, iv) no slip condition near vehicle surface and v) inviscid fluid flow conditions near lateral sidewalls, roof and road or surface of wind tunnel. Table 1 and 2 illustrates the solver setting and model settings used in CFD simulation.

Table 1: Solver Settings

CFD Simulation type	3D
Solver	ANSYS Fluent v14 (Non Commercial Version)
Formulation	Implicit
Time	Steady State
Velocity Formulation	Absolute
Gradient Options	Cell based
Porous Formulation	Superficial Velocity

Table 2: Model Settings

Turbulence Model	Realizable K-epsilon (2 equations)
K-epsilon Model	Realizable
Near wall treatment	Non-equilibrium wall function
Operating Conditions	Ambient

4.2 K-epsilon (K-Ɛ) Model

The K-epsilon model is proposed by Launder and Spalding which is one of the most widely used turbulence models by automobile design engineers *(Launder and Spalding, 1974).* The model is composed of two transport equations which represents the turbulent fluid flow characteristics. It uses eddy viscosity approach to model the Reynolds stresses. History effects (convection and diffusion of turbulent energy) are also taken into account *(Launder and Spalding, 1974)* in this model. The turbulent kinetic energy, K and turbulent dissipation, Ɛ are the first and second transported variables which determine the turbulence energy and scale of turbulent fluid flow, respectively. The model also provides an alternative method for moderate to highly complex fluid flow which earlier used to algebraically prescribe the turbulent length scales *(Jones et al., 1972; Launder and Sharma, 1974).* It was in fact introduced in order to improve the mixing-length model. K-Ɛ model is found to be useful in case of i) free-shear layer flow conditions with small pressure gradients and ii) wall-bounded and internal fluid flows. It is observed that with increase in pressure gradient, accuracy reduces drastically *(Bardina et al., 1997).*The main advantage of K-Ɛ model is that the implementation is relatively simple and easier to converge to the solution with reasonable predication. Though, it too has some shortcomings: i) it is valid only for fully turbulent flows, ii) mandatory implementation of wall functions, iii) Poor flow predication in case of swirling and rotating flow with strong separation *(CD-adapco website; Karthik, 2011)* and iv) unable to perform well under large and adverse pressure gradients *(Wilcox, 2006)*. Keeping in view of the demerits of the existing standard K-Ɛ model, in the present study realizable K-Ɛ model has been considered by author.

4.3 Realizable K-epsilon (K-Ɛ) Model

It is an improved version of existing standard K-Ɛ model *(Shih et al., 1995)*. It consists of a new formulation for the turbulent viscosity along with a new transport equation for the dissipation rate, **Ɛ**. It is derived from the exact equation for transportation of the mean-square vorticity fluctuation. It also satisfies certain mathematical constraints on the Reynolds stresses which are regularly associated with physics of turbulent fluid flow. Main advantages of realizable K-Ɛ model are: i) improved predictions of the spreading rate in case of both planar and round jets, ii) improved performance in case of fluid flow involving rotation and recirculation under strong adverse pressure gradients and iii) ability to capture details of fluid flow over the complex structures *(CD-adapco website; Karthik, 2011)*. Based on the above mentioned discussions, the subsequent solver setting conditions are illustrated in Table 3-8 for ease of simulation.

Table 3: Boundary Conditions at Velocity Inlet

Velocity Inlet	**Velocity magnitude (m/s)**	27.778 (steady and measured along normal direction to the boundary)
	Turbulence Specification Method	Intensity and viscosity Ratio
	Turbulence Intensity	1%
	Turbulence viscosity Ratio	10

Table 4: Boundary Conditions at pressure-outlet

Pressure outlet	**Gauge pressure magnitude (Pascal)**	0
	Gauge pressure direction	Normal to boundary
	Turbulence specification method	Intensity and viscosity ratio
	Backflow turbulence intensity	5%
	Backflow turbulent viscosity ratio	10

Table 5: Wall zone conditions

Base model car surface	No slip wall boundary conditions
Road surface	Inviscid wall boundary conditions
Side walls	Inviscid wall boundary conditions

Table 6: Fluid properties of air

Fluid properties of air	**Material type**	Fluid
	Fluent fluid material	Air
	Density (kg/m^3)	1.225
	Kinematic Viscosity (kg/m-s)	1.7894×10^{-5}

Table 7: Solution Methods

Pressure-velocity coupling scheme		Coupled
Spatial discretization	**Gradient**	Least squares cell based
	Pressure	Standard
	Momentum	Second order upwind
	Turbulent kinetic energy	Second order upwind
	Turbulent dissipation rate	Second order upwind
Convergence Criterion	**Continuity**	10^{-3}
	X-velocity	10^{-3}
	Y-velocity	10^{-3}
	turbulent kinetic energy, K	10^{-3}
	turbulent dissipation, Ɛ	10^{-3}

Table 8: Solution Controls

Flow courant number		50
Explicit relaxation factors	**Momentum**	0.25
	Pressure	0.25
Under relaxation factors	**Density**	1
	Body forces	1
	Turbulent kinetic energy	0.8
	Turbulent dissipation rate	0.8
	Turbulent viscosity	0.95

Energy equation is not taken into consideration as there is no thermal activity due to fluid flow. Coupled scheme is used as iterative algorithm in present study due to its robustness and efficient single phase implementation in case of steady state fluid flow.

5. RESULTS AND DISCUSSION

The results of different passive drag reduction techniques using CFD simulations have been discussed below in brief.

5.1 CFD Simulation of Base model car

The pressure coefficient plot of base model car without using any passive drag reduction techniques clearly indicates that the value of pressure coefficient overshoots at stagnation point in front section of a car as shown in Figs. 6(a) and 6(b).

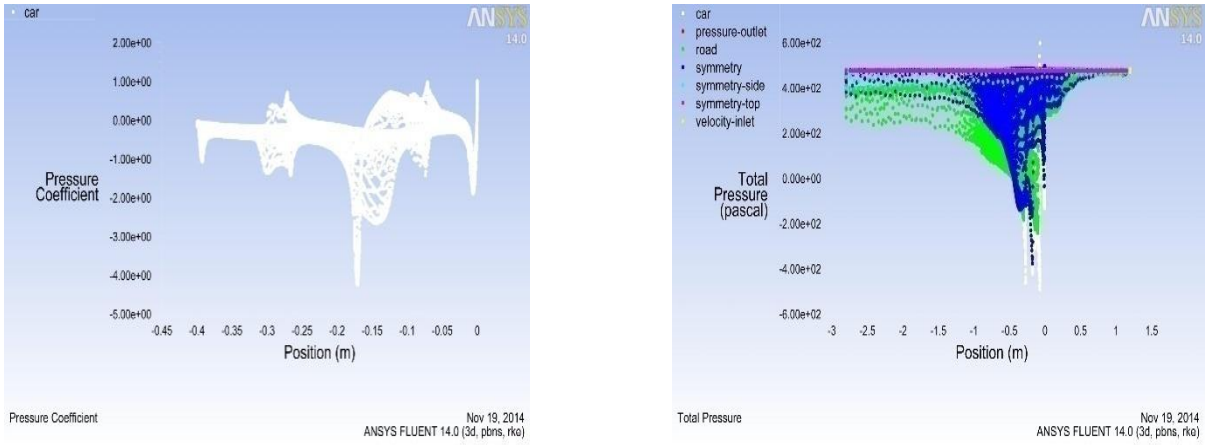

(a) **(b)**

Fig 6: (a) Pressure Coefficient on base model car surface and (b) Total pressure on base model car surface, velocity inlet, pressure outlet, symmetry-side wall, symmetry-top wall and road

Figs. 7(a) and 7(b) depicts the magnitude of drag and lift coefficients (0.33846 and 0.25313) of base model car after successfully fulfilling the convergence criteria respectively.

(a) **(b)**

Fig 7: (a) Drag coefficient and (b) Lift Coefficient of base model car

Figs. 8(a) and 8(b) clearly indicates that there is an increase in negative pressure and generation of large number of vortices at rear section of base model car. Therefore, we need to concentrate on redesigning of the rear section of the car such that flow separation phenomenon is eliminated or minimized.

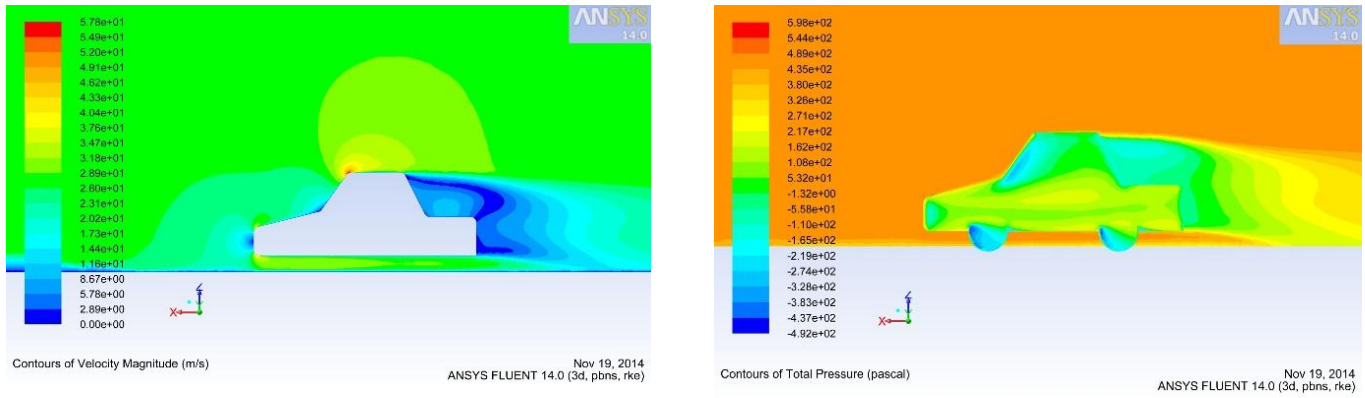

(a) **(b)**

Fig 8: (a) Velocity contour and (b) Total pressure contour of base model car

5.2 CFD Simulation of base model car with passive drag reducing devices

It is general tendency in automobile industry that multiple types of passive drag reducing technologies are used at the same time. Therefore, in the current study, multiple passive drag reducing techniques have been used on our base model car as discussed in subsequent sections.

5.2.1 Rear Tail Plates

The main purpose of rear tail plates is to reduce turbulent intensities in near wake zones, shortening and weakening of recirculation zones and reduction in base pressure by sudden upward deflection of air flowing underneath the car. Angle of attack of rear tail plates has large influence on magnitude of drag coefficient. The base model car is fitted with rear tail plate of 25 mm length (reduced scale) at 20° angle of attack as illustrated in Fig. 9(a) and 9(b).

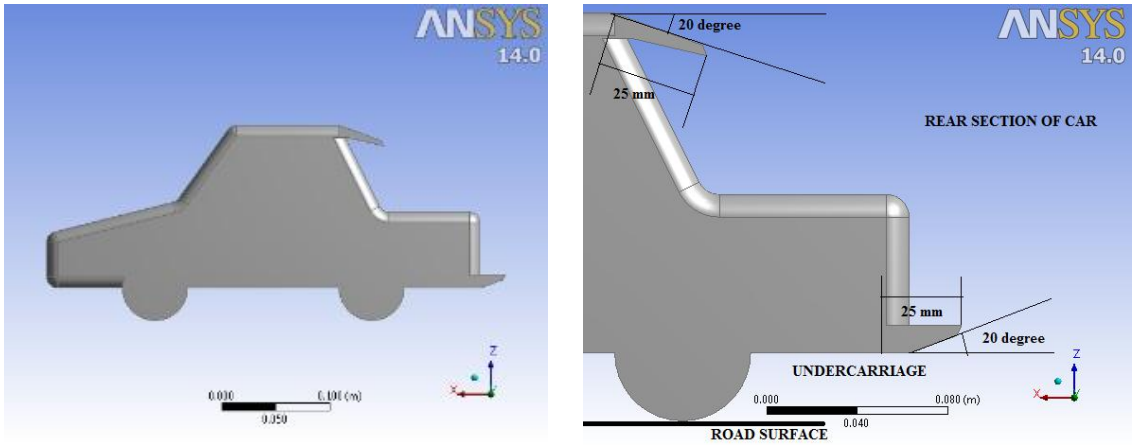

(a) Overall system **(b) Installation details**

Fig 9: Base model car fitted with rear tail plate at 20° angle of attack

5.2.2 Ground Effect with Rear Tail Plate

The base model car front and rear end ground clearance has been reduced by 50% and increased by 25% with respect to reference design respectively along with rear tail plate of 25 mm length (reduced scale) installed on car roof at an angle of attack of 20° as shown in Fig. 10(a) and 10(b) to facilitate large pressure differential across top and bottom sections of the car for improving dynamic stability.

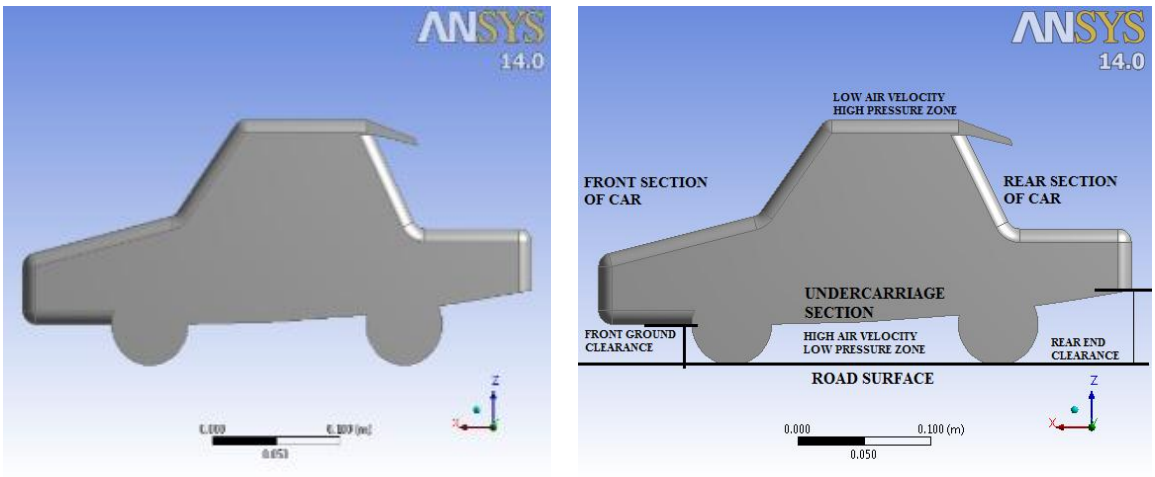

(a) Overall System **(b) Geometrical configuration**

Fig 10: Base model car with undercarriage unit modified for Ground effect and fitted with rear tail plate at 20° angle of attack in rear section of car roof

5.2.3 Diffuser with Rear Tail Plate

The front ground clearance has been reduced by 75% with respect to earlier design with the inclusion of elevation angle of 5° starting from point located at 0.5L from front section of the base model car in undercarriage unit along with rear tail plate of 25 mm length (reduced scale) installed on car roof at an angle of attack of 20° as illustrated in Fig. 11(a) and 11(b) to facilitate the development of high pressure zones underneath the car.

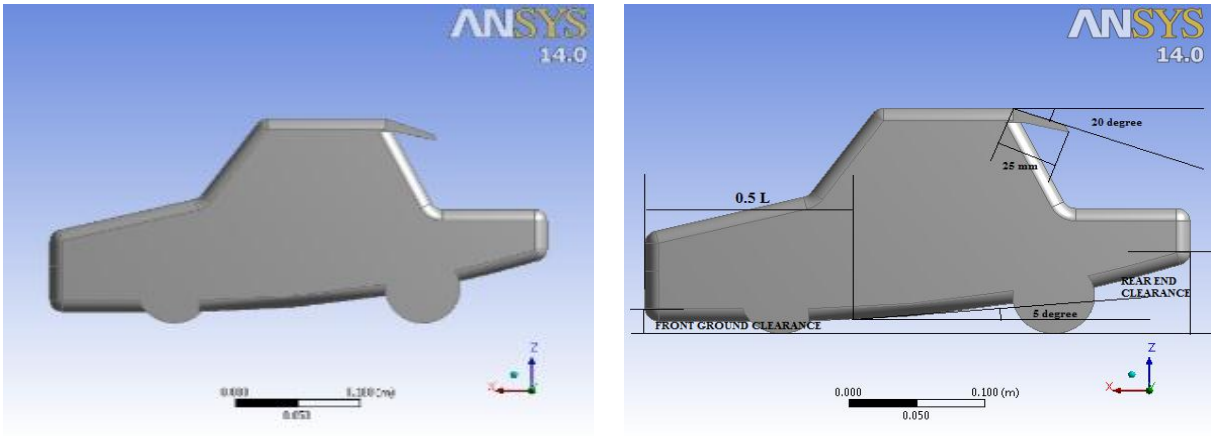

(a) Overall System **(b) Geometrical configuration**

Fig 11: Base model car with undercarriage modified into diffuser and fitted with rear tail plate at 20° angle of attack in rear section of car roof

5.2.4 Front Bonnet Duct with Rear Tail Plate and Diffuser

It has been installed over bonnet of base model car at an elevation angle of 26.565° along with diffuser and rear tail plate similar to that of discussed earlier as depicted in Fig. 12(a) and 12(b) to reduce the formation of high pressure zones in front section of a car. Earlier, this technique has merely implemented for improving the air intake of engine. Elevation angle of front bonnet duct facing the wind screen has been designed in such a way that at least half of the air flow is directed away from front wind screen. It reduces the drag coefficient by preventing stagnation of air flow.

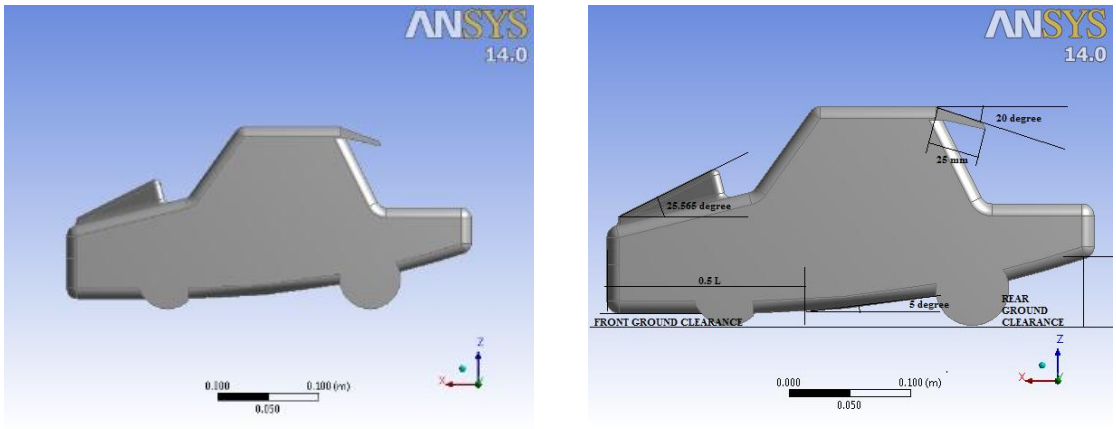

(a) Overall System **(b) Geometrical configuration**

Fig 12: Base model car fitted with front bonnet duct, diffuser and rear tail plate at 20° angle of attack in rear section of car roof

5.2.5 Rear Spoilers with Rear Tail Plate and Diffuser

It has been installed in the rear section of the base model car at an angle of attack of 26.565° with leading and trailing edge located at the heights of 60 and 80 mm (reduced scale), respectively along with diffuser and rear tail plate similar to that of discussed earlier as illustrated in Fig. 13(a) and (b). It is used to generate enormous amount of negative lift forces with little increment in drag coefficient. While designing the rear spoiler, care must be taken regarding angle of attack to generate strong negative lift forces. The height of installation of the rear spoiler must be equal to the vertical height of the rear wind screen

which provides the least diverted air stream to the rear spoiler thereby producing ground effect by developing high pressure zone under the rear spoiler.

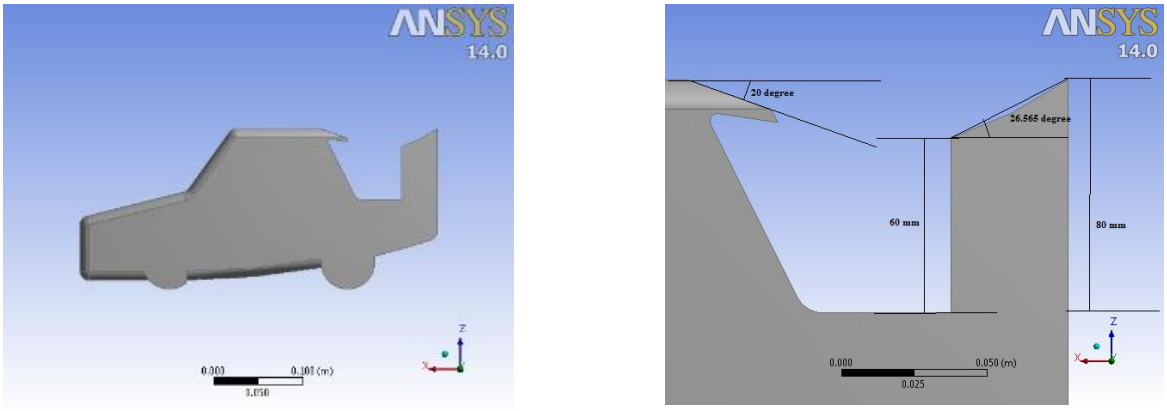

(a) Overall System **(b) Installation setup of rear spoiler**

Fig 13: Base model car fitted with rear spoiler, diffuser and rear tail plate at 20° angle of attack in rear section of car roof

5.2.6 Vortex Generator

The trailing edge of the base model car roof has been fitted with 10 mm long and 25 mm height (reduced scale) vortex generators at an angle of attack of 18° as shown in Figs. 14 and 15 to reduce the development of high pressure zones near rear wind screen. Though, this technique not only reduces a good amount of drag coefficient but also induces small amount of drag simultaneously.

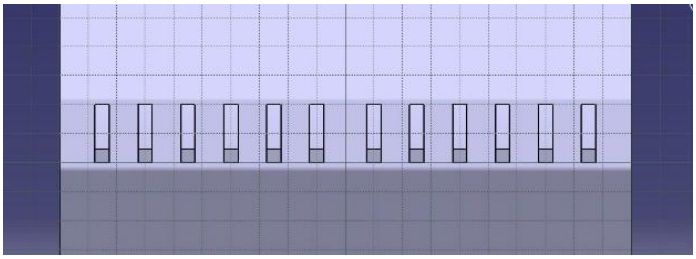

Fig 14: Top view of vortex generators installed on end of base model car roof

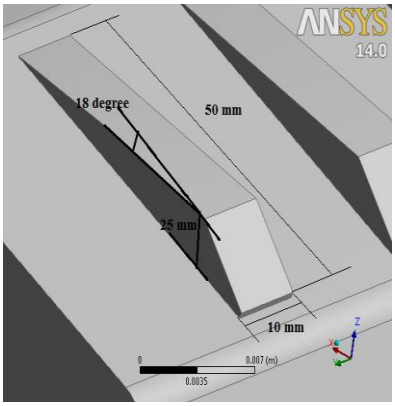

Fig 15: Geometrical configuration of vortex generator (h = 25 mm, reduced scale)

5.2.7 Rear fairing

The shape of rear fairing has been taken similar to that of truncated cone with rectangular base as shown in Fig. 16(a) and 16(b). It has minimum to maximum slant angle from 19° to 25° starting from beginning of rear wind screen to rear end and rear wheel to rear end of the base model car. It minimizes flow separation phenomenon occurring at the rear section.

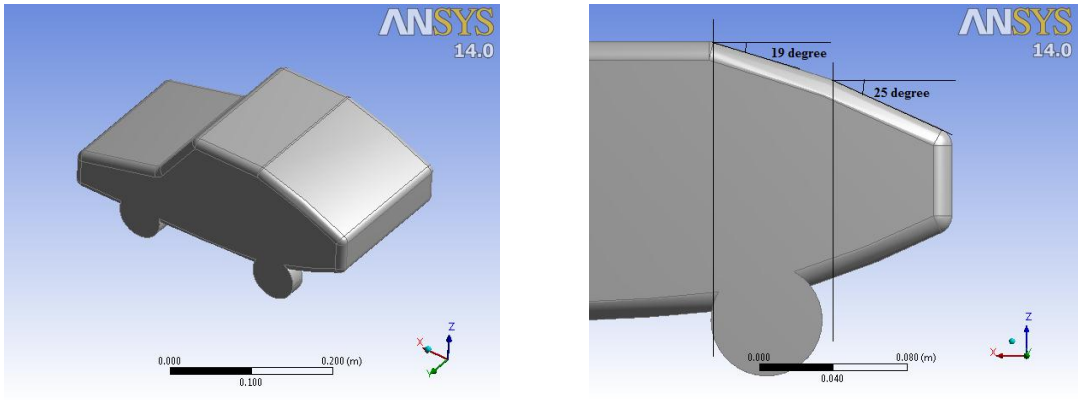

(a) Overall System **Geometrical configuration**

Fig. 16: Base model car with rear fairing

The computation process was done till solution converges after implementing the boundary condition as stated in Tables 3-8 while running ANSYS Fluent v-14. As a part of post-processing component, graphical plots showing convergence of magnitudes of drag (C_d) and lift (C_l) coefficients during computation process are illustrated in Fig. 17 after installing the above mentioned passive drag reduction devices/techniques. Similarly, the velocity and pressure contours are depicted in Fig. 18.

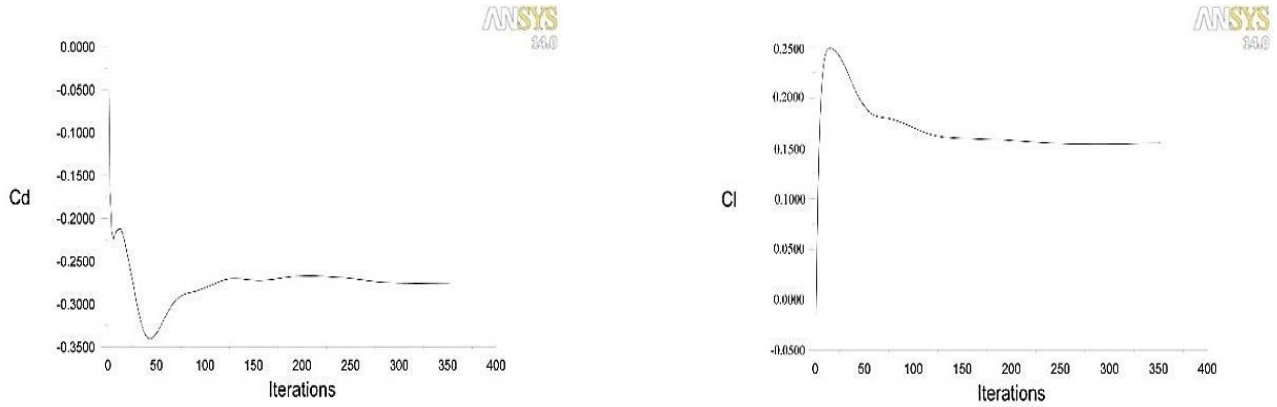

(a) **(b)**

(a) Drag Coefficient and (b) Lift Coefficient of the base model car fitted with rear tail plate at 20° angle of attack

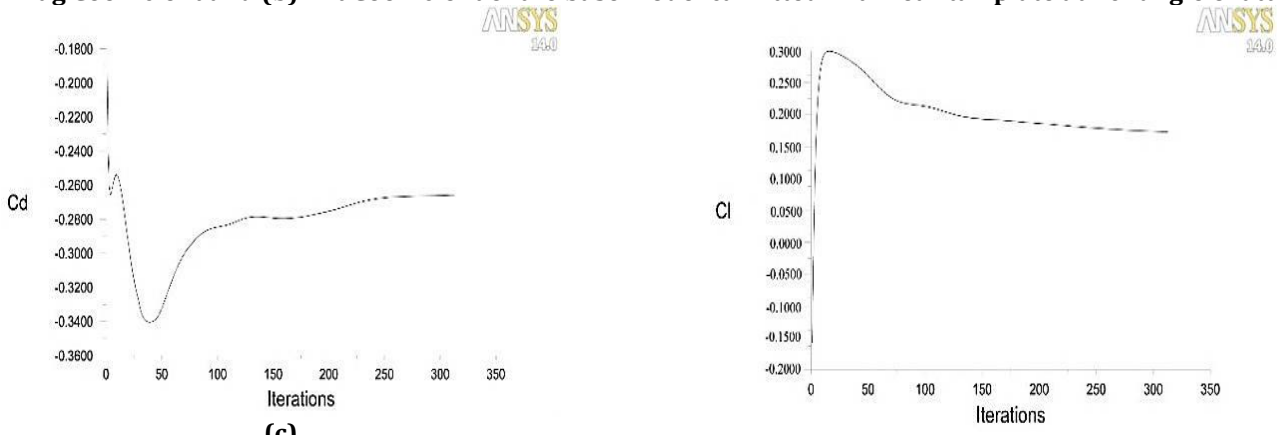

(c) **(d)**

(c) Drag Coefficient and (d) Lift Coefficient of the base model car with undercarriage unit modified for Ground effect and fitted with rear tail plate at 20° angle of attack in rear section of car roof

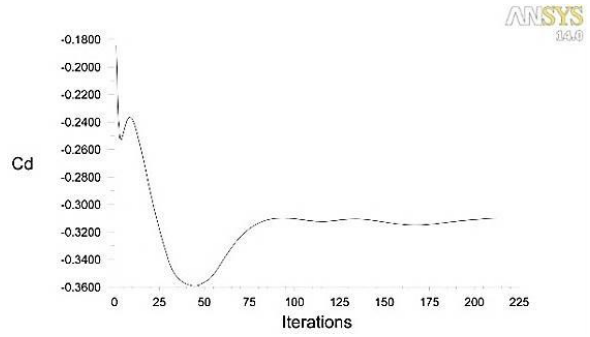

(e)

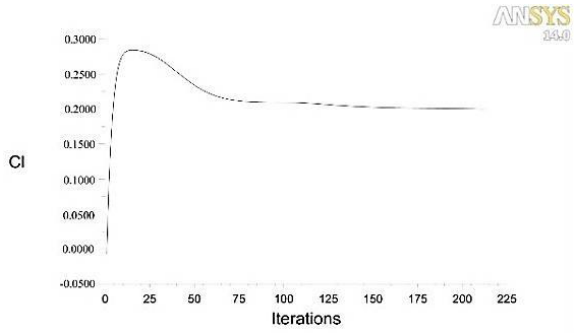

(f)

(e) Drag Coefficient and (f) Lift Coefficient of the base model car with undercarriage modified into diffuser and fitted with rear tail plate at 20° angle of attack in rear section of car roof

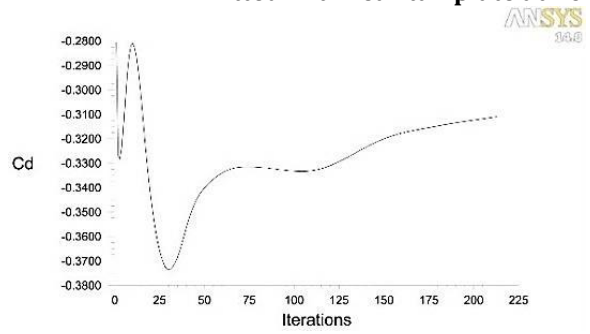

(g)

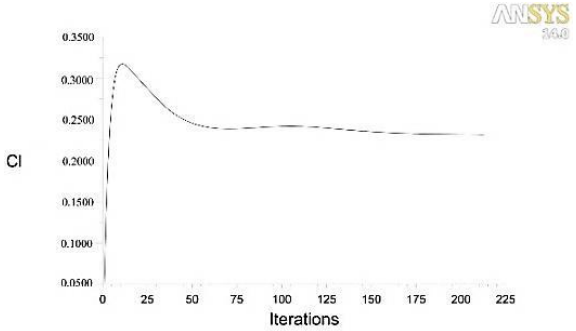

(h)

(g) Drag Coefficient and (h) Lift Coefficient of the base model car fitted with front bonnet duct, diffuser and rear tail plate at 20° angle of attack in rear section of car roof

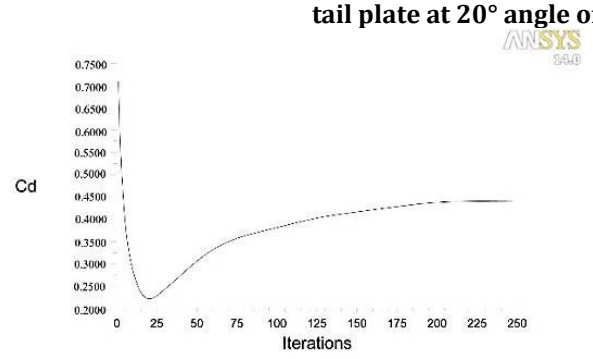

(i)

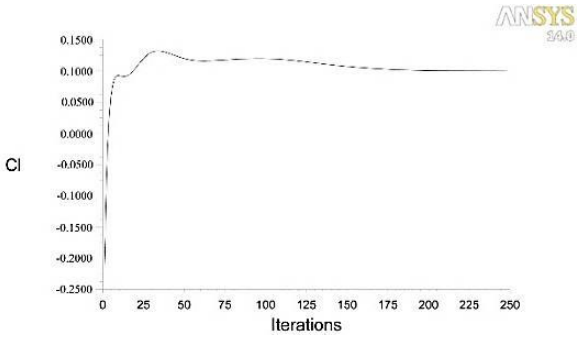

(j)

(i) Drag Coefficient and (j) Lift Coefficient of the base model car fitted with rear spoiler, diffuser and rear tail plate at 20° angle of attack in rear section of car roof

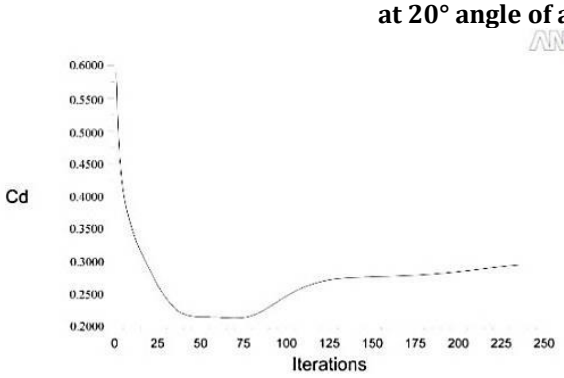

(k)

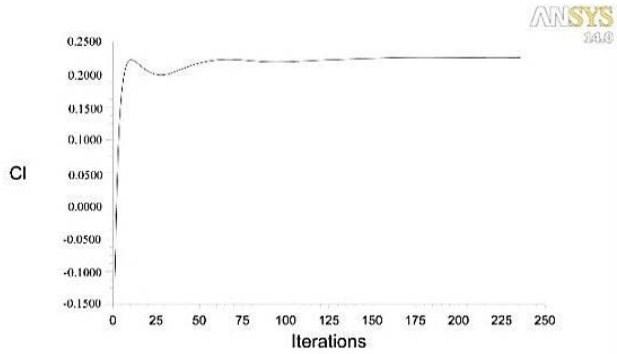

(l)

(k) Drag Coefficient and (l) Lift Coefficient of the base model car fitted with vortex generators

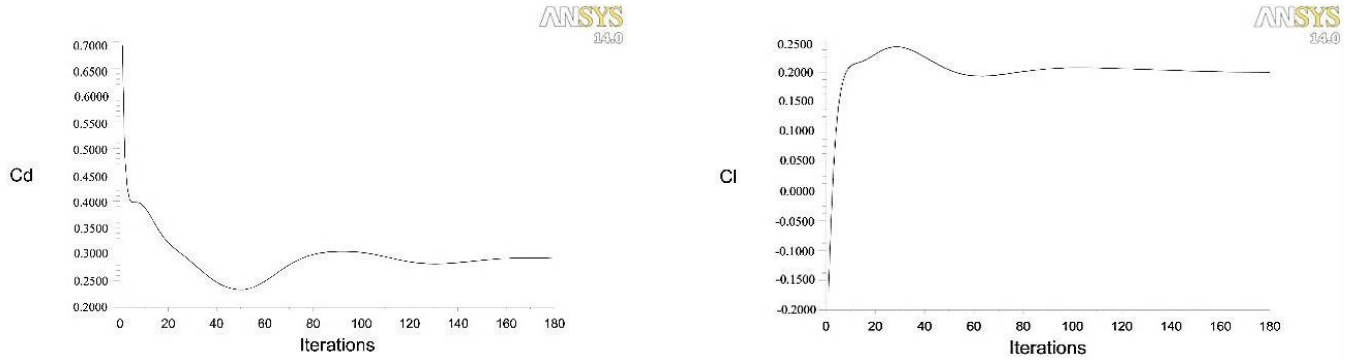

(m) (n)

(m) Drag Coefficient and (n) Lift Coefficient of the base model car fitted with rear fairing

Fig. 17: Plots illustrating convergence of drag and lift coefficients as per convergence criteria for various passive drag reducing devices which are installed in base model car

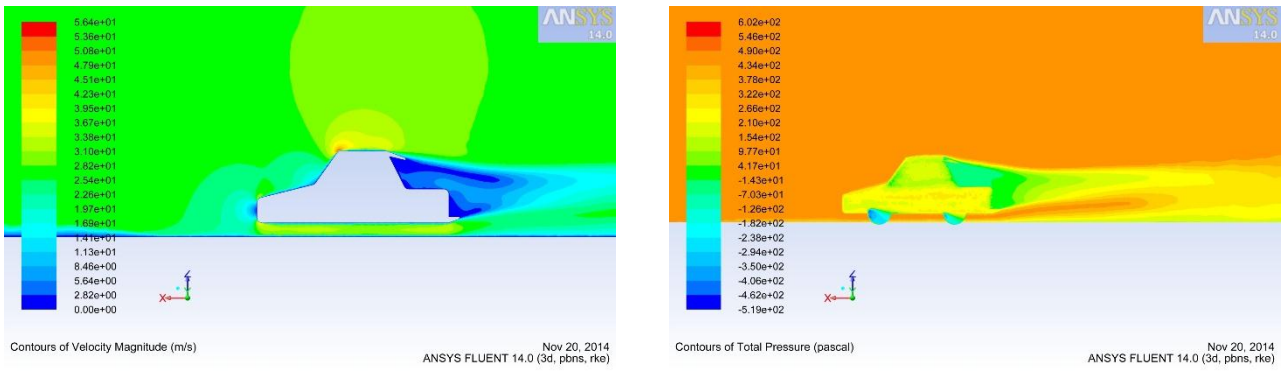

(a) (b)

(a) Velocity contour and (b) Total pressure contour of the base model car fitted with rear tail plate at 20° angle of attack

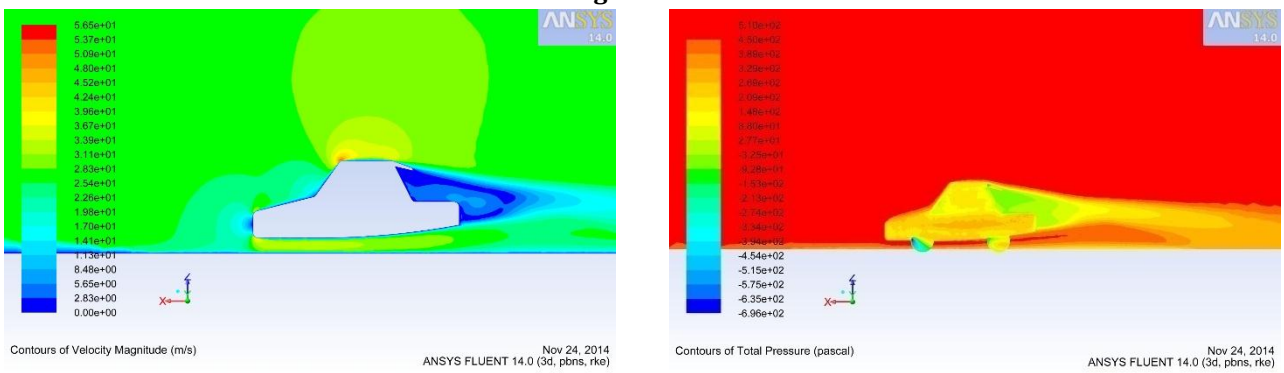

(c) (d)

(c) Velocity contour and (d) Total pressure contour of the base model car with undercarriage unit modified for Ground effect and fitted with rear tail plate at 20° angle of attack in rear section of car roof

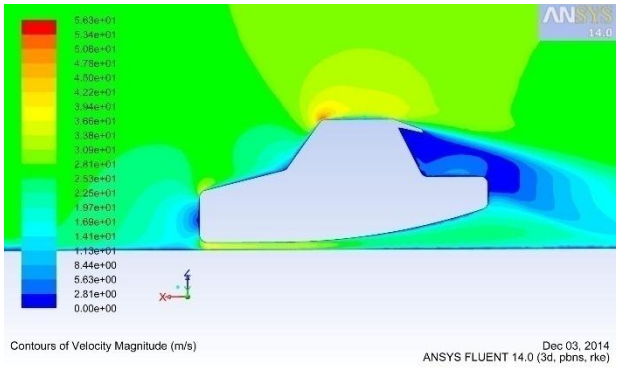

(e)

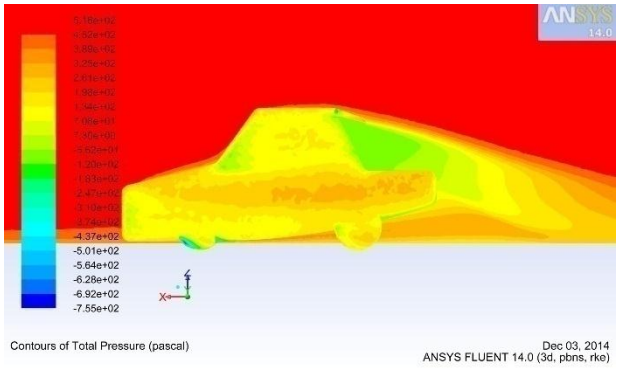

(f)

(e) Velocity contour and (f) Total pressure contour of the base model car with undercarriage modified into diffuser and fitted with rear tail plate at 20° angle of attack in rear section of car roof

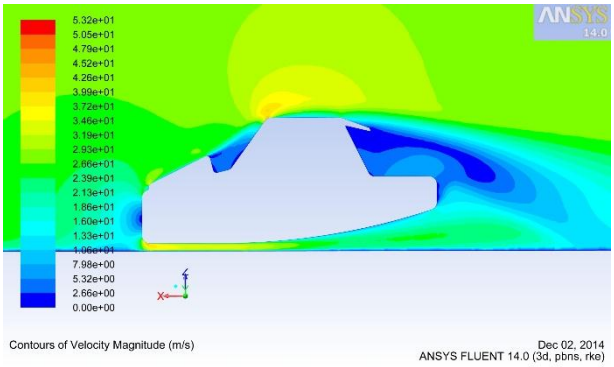

(g)

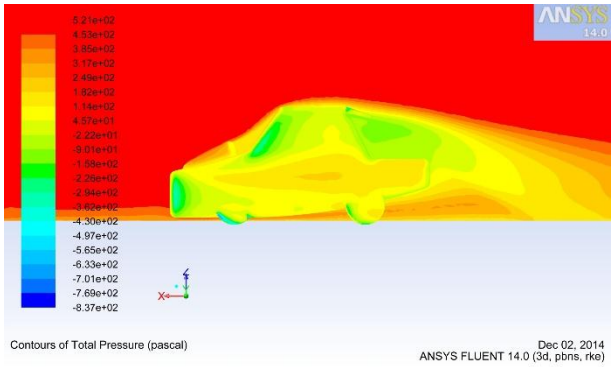

(h)

(g) Velocity contour and (h) Total pressure contour of the base model car fitted with front bonnet duct, diffuser and rear tail plate at 20° angle of attack in rear section of car roof

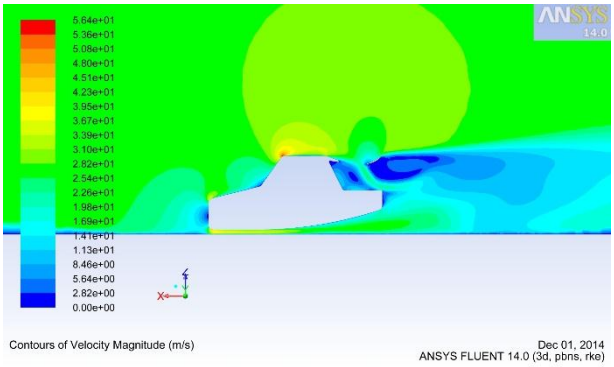

(i)

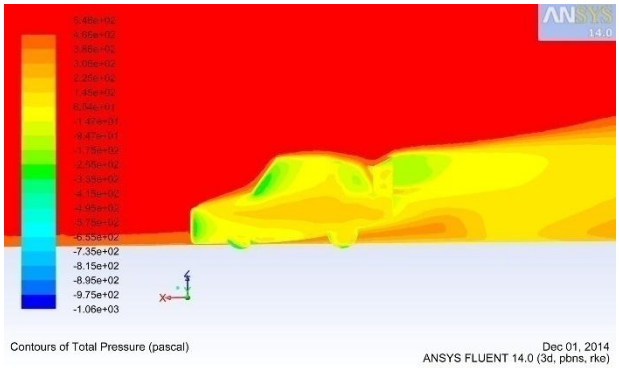

(j)

(i) Velocity contour and (j) Total pressure contour of the base model car fitted with rear spoiler, diffuser and rear tail plate at 20° angle of attack in rear section of car roof

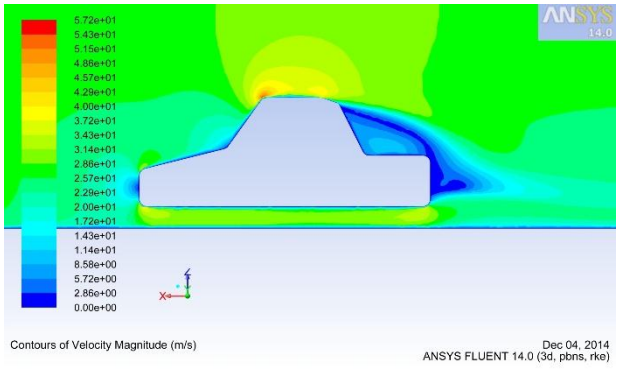

(k)

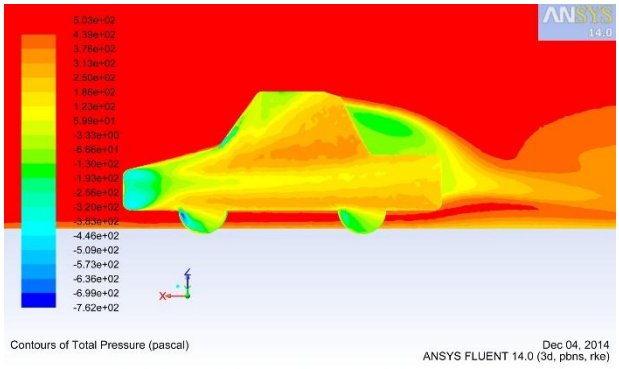

(l)

(k) Velocity contour and (l) Total pressure contour of the base model car fitted with vortex generators

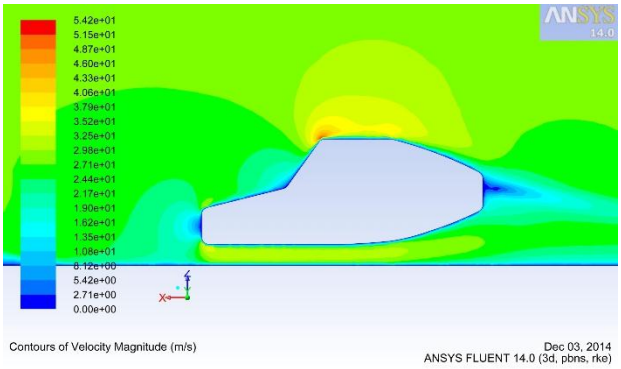

(m)

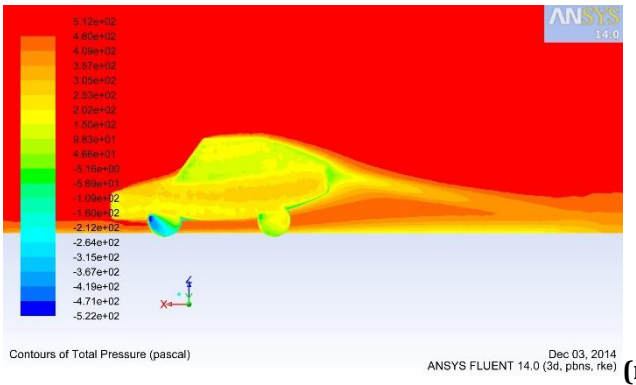

(n)

(m) Velocity contour and (n) Total pressure contour of the base model car fitted rear fairing

Fig. 18 : List of velocity and pressure contours of various passive drag reducing devices which are installed in base model car

6. CONCLUSION

The external vehicle aerodynamic characteristics of base model car attached with various passive drag reducing devices/techniques have been studied using ANSYS Fluent v14 in this paper. The comparison of effect of installation of such devices on the base model car has been shown in Table 9 in terms of magnitudes of drag and lift coefficients. The velocity and total pressure contour of base model car clearly indicate that the installation of such devices has great influence on i) wake zone formation, ii) streamlining of fluid flow over the car surface and iii) reducing air recirculation with minimized zone of flow separation behind rear section of a car.

Table 9: Drag and Lift Coefficient of Base model car and Base model car fitted with passive drag reducing devices

DESIGN CONFIGURATION	DRAG COEFFICIENT (C_d)	LIFT COEFFICIENT (C_l)	% CHANGE IN C_d	% CHANGE IN C_l
Base Car model without any passive drag reducing technology	0.33846	0.25313	Not Applicable	Not Applicable
BASE CAR MODEL WITH PASSIVE DRAG REDUCING TECHNOLOGY				
Rear tail flaps (20° angle of attack)	0.27604	0.15625	−18.442	−38.272
Ground Effect with rear tail plate (20° angle of attack)	0.26569	0.16250	−21.500	−35.803
Diffuser (ground clearance reduced by half) with	0.30988	0.20313	−8.444	−19.753

rear tail plate (20° angle of attack)				
Front bonnet Duct (26.565° elevation angle) fitted with diffuser and rear tail plate (20° angle of attack)	0.31099	0.23750	−8.116	−6.175
Rear Spoilers fitted with diffuser and rear tail plate (20° angle of attack)	0.40313	0.10078	+19.107	−60.186
Vortex Generator	0.29375	0.20625	−13.209	−18.520
Rear fairing	0.28750	0.18750	−15.056	−25.927
Note: + and− signs indicate increment and decrement in values of C_d and C_l				

Hence, Installation of such passive drag reducing technologies either individually or in combination would help in improving fuel consumption and dynamic stability of base model car by reducing aerodynamic drag in cost efficient manner in comparison to active drag reducing technologies.

REFERENCES

1) Ahmad, N. E.,Abo-Serie, E. and Gaylard, A., Mesh Optimization for Ground Vehicle Aerodynamics, CFD Letters, Vol. 2(1), pp54-65, 2010.
2) Ahmed, H. and Chacko, S., Computational optimization of vehicle aerodynamics, Proceedings of the 23rd International DAAAM Symposium, Volume 23(1), pp 313-318, 2012.
3) Altaf, A., Omar, A. A. and Asrar, W., Review of passive drag reduction techniques for bluff road vehicles, IIUM Engineering Journal, Vol. 15(1), pp 61-69, 2014.
4) Bardina, J.E., Huang, P.G., Coakley, T.J. , Turbulence Modeling Validation, Testing, and Development , NASA Technical Memorandum 110446, pp1-85, 1997.
5) Buchholz, K., Lightweight Body Panel Materials, Automotive Engineering International, Vol. 106(12), pp19-22, 1998.
6) Carr, G.W., The Study of Road Vehicle Aerodynamics Using Wind Tunnel Models, In Proc. 1st Symp. Road Vehicle Aerodynamics, London, pp1-14, 1969.
7) Chainani, A. and Perera, N., CFD Investigation of airflow on a model radio control race car, In Proc. of the World Congress on Engineering-London, Vol II, pp1588-1591, 2008.
8) Daryakenari, B., Abdullah, S., Zulkifli, R., Sundararajan, E., and Sood, A. M., Numerical study of flow over Ahmed body and a road vehicle and the change in aerodynamic characteristics caused by rear spoiler, International Journal of Fluid Mechanics Research, Vol.40(4), pp354-372, 2013.
9) Demmler, A., Trends in Automotive Materials, Automotive Engineering International, pp. 26 -27, 1998.
10) Dubey, A., Chheniya, S., and Jadhav, A., Effect of Vortex generators on Aerodynamics of a Car: CFD Analysis. International Journal of Innovations in Engineering and Technology (IJIET), Vol. 2(1), pp137-144, 2013.
11) Fourrié, G., Keirsbulck, L., Labraga, L., and Gilliéron, P., Bluff-body drag reduction using deflector, Experiments in Fluids, Vol.50 (2), pp385-395, 2011.
12) Hsu, F. H. and Davis, R. L., Drag reduction of tractor-trailers using optimized add-on devices, Journal of Fluids Engineering, pp132-140, 2010.
13) http://www.cd-adapco.com/sites/default/files/technical_document/pdf/PRU_2012.pdf (assessed on 10th Dec 2018).
14) Hu, X. X., and Wong, T. T., A numerical study on rear-spoiler of passenger vehicle, World Academy of Science, Engineering and technology, Vol. 57, pp636-641, 2011.
15) Hucho, W. H. and Sovran, G., Aerodynamics of road vehicles, Annual Review of Fluid Mechanics, Vol. 25(1), pp485-537, 1993.
16) Huminic, A., Huminic, G., and Soica, A., Study of aerodynamics for a simplified car model with the underbody shaped as a venturi nozzle, International Journal of Vehicle Design, Vol.58(1), pp15-32, 2012.
17) Jones, W. P., and Launder, B. E., The Prediction of Laminarization with a Two-Equation Model of Turbulence, International Journal of Heat and Mass Transfer, Vol. 15, pp301-314, 1972.
18) Karthik, T.S.D., IIT Madras, Turbulence models and their applications,10th Indo German Winter Academy,pp1-52,2011(www.leb.eei.uni-erlangen.de/winterakademie/2011/report/content/course01/pdf/0112.pdf) (assessed on 10th Dec 2018).
19) Katz, J., Aerodynamics of Race Cars, The Annual Review of Fluid Mechanics, pp27-63, 2006.
20) Khalighi, B., Balkanyi, S. R., and Bernal, L. P., Experimental investigation of aerodynamic flow over a bluff body in ground proximity with drag reduction devices, International Journal of Aerodynamics, Vol.3(4), pp217-233, 2013.
21) Koike, M., Nagayoshi, T., Hamamoto, N., Research on Aerodynamic Drag Reduction by Vortex Generators, Mitsubishi Motors Technical Review, No 6, pp1-16, 2004.

22) Launder, B. E., and Sharma, B. I., Application of the Energy Dissipation Model of Turbulence to the Calculation of Flow Near a Spinning Disc", Letters in Heat and Mass Transfer, Vol. 1(2), pp131-138, 1974.
23) Launder, B.E. and Spalding, D.B.,The numerical computation of turbulent flows, Computer Methods for Applied Mechanics & Engineering, Vol. 3, pp. 269-89, 1974.
24) Majumder, S. and Saha, S., A method of drag reduction of a vehicle by computational investigation and Geometric modification, International journal of Applied Engineering Research, Vol. 9(6), pp 687-689, 2014.
25) Marklund, J., Lofdahl, L., Danielsson, H., and Olsson, G., Performance of an automotive under-body diffuser applied to a sedan and a wagon vehicle, SAE International Journal of Passenger Cars-Mechanical Systems, Vol. 6(1), pp293-307, 2013.
26) Mayer, W. and Wickern, G., The new audi A6/A7 family-aerodynamic development of different body types on one platform, SAE International Journal of Passenger Cars-Mechanical Systems, Vol. 4(1), pp197-206, 2011.
27) Mazyan, W. I., Numerical simulations of drag reducing devices for ground vehicles, Master of Science in Mechanical Engineering dissertation, American University of Sharjah, pp1-85, 2013.
28) Rohatgi, U. S., Methods of Reducing Vehicle Aerodynamic Drag, ASME Summer Heat Transfer Conference (Puerto Rico, USA), pp1-8, 2012.
29) Sharma, R. B., and Bansal, R., CFD simulation for flow over passenger car using tail plates for aerodynamic drag reduction, IOSR Journal of Mechanical and Civil Engineering (IOSR-JMCE), Vol. 7(5), pp 28-35, 2013.
30) Shih, T. H., Liou, W. W., Shabbir, A., Yang, Z. and Zhu, J., A New K- Ɛ Eddy Viscosity Model for High Reynolds Number Turbulent Flows—Model Development and Validation. Computers Fluids, Vol 24(3), pp227-238, 1995.
31) Singh, S. N., Rai, L. and Bhatnagar A., Effect of moving surface on the aerodynamic drag of road vehicles, Proceeding of IMechE., pp127- 134, Vol. 219 , 2004.
32) Skaperdas, E. and Kolovos, C., Automated pre-processing for high quality multiple variant CFD models of a city class car, 3rd ANSA & µETA International Conference, pp1-15, 2009.
33) Small, Kenneth, A., and Dender, K. V., Fuel Efficiency and Motor Vehicle Travel: The Declining Rebound Effect, Energy Journal, Vol. 28(1), pp25–52, 2006.
34) Sudin, M. N., Abdullah, M. A., Shamsuddin, S. A., Ramli, F. R. and Tahir, M. M., Review of Research on Vehicles Aerodynamic Drag Reduction Methods, International Journal of Mechanical & Mechatronics Engineering (IJMME-IJENS), Vol. 14(2) , pp35-47, 2014.
35) Wahba, E. M., Al-Marzooqi, H., Shaath, M., Shahin, M. and El-Dhmashawy, T., Aerodynamic Drag Reduction for Ground Vehicles using Lateral Guide Vanes, CFD Letters, pp 68-79, Vol. 4 (2), June 2012.
36) Wilcox, D. C., Turbulence Modeling for CFD (Third edition), D C W Industries Publications, pp1-522, 2006.
37) Xingjun Hu, Bo Yang, Zing-Yu Wang and Ting Li., Research on influences of rear-view mirror on aerodynamic drag characteristics of truck. Journal of Human University Natural Sciences, pp65-69, 2010.
38) Xingjun Hu, Peng Qin, Peng Guo and Yang, An Effect of turbulence parameters on numerical simulation of complex automotive external flow field. Applied Mechanics and Materials, pp1062-1067, 2011.
39) Zake, R. B. C., Aerodynamics of aftermarket rear spoiler, Bachelor of Mechanical Engineering with Automotive Engineering Thesis, Faculty of Mechanical Engineering, University Malaysia Pahang, pp1-39, 2008.

BIOGRAPHIES

Mr. Basudev Datta has 4+ years of experience in R&D and Teaching Sector. He has worked as Assistant Professor in Department of Mechanical Engineering, C V Raman College of Engineering-Bhubaneswar and Trainee Scientist (Scientist Gr.IV(1)) in CSIR-Central Institute of Mining and Fuel Research, Dhanbad. He has completed Bachelor of Engineering in Mechanical Engineering Stream from Visvesvaraya Technological University-Belgaum and Master of Technology in Mine Safety Engineering Stream from Academy of Scientific and Innovative Research-New Delhi (An Institute of National Importance). He is a Gold Medalist and recipient of many accolades during his UG and PG. During his tenure in CSIR, he was engaged in various CSIR Labs network projects sanctioned under 12th Five Year Planning Commission Committee (2012-2017). He has published 5 research papers in International Conference & Journals till date. He is currently pursuing MBA in Operations Management from Symbiosis Institute of Management Studies-Pune.

Mr. Vaibhav Goel is currently pursuing B.Tech. in Mechanical Engineering Stream from Chitkara University Institute of Engineering &Technology-Rajpura. He has extensive hand-on experience in Automobile Engineering, Operations Management, Production Engineering and Robotics through various mini-projects.

Mr. Shivam Garg is currently pursuing B.Tech. in Mechanical Engineering Stream from Chitkara University Institute of Engineering &Technology-Rajpura. He has extensive hand-on experience in CAD tool such as AutoCAD, Tribology, Automobile Engineering and Robotics through various mini-projects.

Mr. Inderpreet Singh is currently pursuing B.Tech. in Mechanical Engineering Stream from Chitkara University Institute of Engineering &Technology-Rajpura. He has extensive hand-on experience in FEA tool such as ANSYS, Composite Materials and Automobile Engineering through various mini-projects.